Thermally Assisted Skyrmion Memory (TA-SKM)

Shijiang Luo, Nuo Xu, *Member, IEEE*, Yaoyuan Wang, Jeongmin Hong, and Long You, *Member, IEEE*

***Abstract*— A novel thermally assisted skyrmion memory (TA-SKM) has been proposed and studied for the first time. Unidirectional current-induced spin transfer torque (STT) and Joule heating effect are used to induce the magnetization switching between uniform and skyrmion states in the free layer of a magnetic tunnel junction device. Physics-based simulations suggest that TA-SKM offers advantages including unipolar switching feature for cross-point memory integration, better TMR design as compared to STT-MRAM, and improved operation temperature range as compared to TA-MRAM.**

***Index Terms*— Skyrmion, thermally assisted magnetic memory, magnetic tunnel junction, spin transfer torque.**

I. Introduction

SPIN transfer torque magnetic random access memory (STT-MRAM) is among the most promising candidates of universal memory technologies due to its low operating power, non-volatility, and compact cell area [1]–[3]. Magnetic tunnel junction (MTJ), as a ferromagnetic (FM) free layer (FL)/barrier layer (BL)/FM pinned layer (PL) structure, is used as the core switch element of an STT-MRAM. Existing STT approach relies on the polarized charge current to transfer spin torques to completely flip the FL's magnetization. Moreover, thermally assisted (TA) magnetic switching shows great promise for developing TA-MRAM [4]–[6] or HAMR [7]–[9] in data storage applications. By taking advantage of the *Joule* heating effect (JHE) produced by current pulse flowing through the MTJ, the FL can be temporarily heated up to a high temperature thus reducing the anisotropy for writing with low current density [6].

On the other hand, magnetic skyrmions, stabilized in FM films contacted with heavy metal (HM), exhibit a non-uniform magnetization distribution with whirling configuration and topological property due to the *Dzyaloshinskii–Moriya* interaction (DMI) existing at FM/HM interface [10]–[15]. Previous studies have shown that an isolated skyrmion can be generated by STT with local injection of spin-polarized current into an FM film [16], [17]. Another approach for skyrmion creation and annihilation via localized heating with laser irradiation has also been proposed [18], [19]. However, creating a skyrmion using STT-only approach requires quite large current density ($J > 10^2$ MA/cm^2), while laser heating approach isincompatible for high density memory integrations.

In this work, through physics-based simulations, we study the skyrmion creation and annihilation controlled by both current-induced STT and heating. Unidirectional SET ($0 \rightarrow 1$) and RESET ($1 \rightarrow 0$) currents are applied to induce a change of the magnetic textures back and forth between uniform and skyrmion states. Therefore, a new kind of memory device is proposed as thermally assisted skyrmion memory (TA-SKM).

II. Device Concept and Simulation Methods

Fig. 1a shows the basic TA-SKM structure studied in this work, which consists of HM layer/FL/BL/PL encapsulated by thermal barrier (TB) layers and can be fabricated similar to a TA-MRAM stack. Both FL and PL have perpendicular magnetic anisotropy (PMA), while HM layer with strong spin-orbit coupling generates interfacial DMI to the FL [20]. PL with a circular shape and smaller than FL is used for local current injection. TBs are inserted on both sides of the MTJ to increase the heating efficiency of FL while maintaining the electrical resistivity of overall stack. Typical metals (*e.g.* Ta [5]) or metal nitrides (*e.g.* TiN, TaN [21]) are best fit for these applications. Unidirectional currents (I) vertically flowing through the stack into the FL to create a skyrmion from a uniform FM state via STT, or increase the FL's temperature (T) via JHE to erase the skyrmion back to uniform magnetization state. The MTJ shows a low resistance state (LRS, "0") with FL in uniform state and a high resistance state (HRS, "1") in skyrmion state, respectively, for memory application.

Magnetization dynamics in FL are simulated under micromagnetic framework using OOMMF [22] with temperature module [23] by numerically solving the stochastic *Landau-Lifshitz-Gilbert* (LLG) equations as [23], [24]

$$\frac{\partial \mathbf{m}}{\partial t} = -\gamma_0 \mathbf{m} \times (\mathbf{H}_{\text{eff}} + \mathbf{H}_{\text{T}}) + \alpha \left(\mathbf{m} \times \frac{\partial \mathbf{m}}{\partial t}\right) + \gamma_0 u (\mathbf{m} \times \mathbf{m} \times \mathbf{p}), \tag{1}$$

where $\mathbf{m}$, t, γ_0, α, and $\mathbf{p}$ are the magnetization, time, gyromagnetic ratio, damping coefficient, and the unit spin-polarization vector of the spin current, respectively. $\mathbf{H}_{\text{eff}}$ is the effective field, considering exchange, uniaxial anisotropy, DMI, and demagnetization. $\mathbf{H}_{\text{T}}$ is the Gaussian thermal fluctuation fields. Last term on the right side represents the STT. The geometrical and material-related parameters are listed in Table I, based on Co/Pt multilayer. Since the skyrmion lifetime decreases exponentially with temperature [25], large PMA (K_{u}) and DMI (D) constant values are selected as compared to commonly

Manuscript received March 15, 2020; revised April 1, 2020; accepted April 2, 2020. Date of publication April 7, 2020; date of current version May 21, 2020. This work was supported in part by the National Natural Science Foundation of China under Grant 61674062. The review of this letter was arranged by Editor B. G. Malm. *(Corresponding author: Long You.)*

Shijiang Luo, Yaoyuan Wang, Jeongmin Hong, and Long You are with the School of Optical and Electronic Information, Huazhong University of Science and Technology, Wuhan 430074, China (e-mail: lyou@hust.edu.cn).

Nuo Xu is with the Department of Electrical Engineering and Computer Sciences, University of California, Berkeley, CA 94720, USA.

Color versions of one or more of the figures in this letter are available online at http://ieeexplore.ieee.org.

Digital Object Identifier 10.1109/LED.2020.2986312

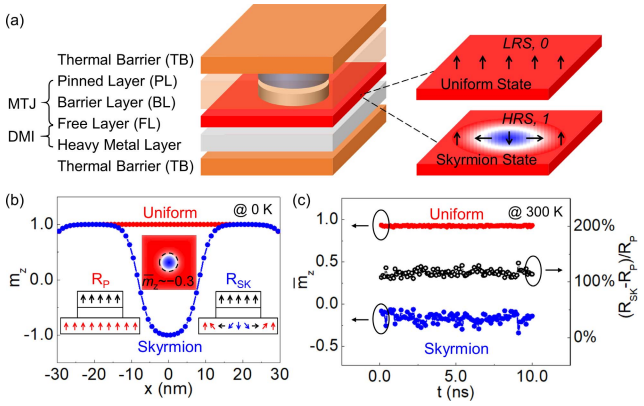

Fig. 1. (a) Schematics of TA-SKM, consisting of heavy metal (HM) layer/free layer (FL)/barrier layer/pinned layer (PL) covered by thermal barriers. HM layer with strong spin-orbit coupling generates interfacial DMI to the FL. MTJ shows a low resistance state (LRS, 0) with free layer in uniform state and a high resistance state (HRS, 1) in skyrmion state. (b) Magnetization distribution of uniform and skyrmion state at 0 K. (c) Time-dependent magnetization of uniform and skyrmion states and the resistance variation $(R_{SK} - R_P)/R_P$ at 300 K. Here, m_z is the normalized perpendicular component of magnetization in the FL, and $\bar{m}_z$ is the average m_z in local area of FL below PL.

TABLE I
SIMULATION PARAMETERS

Parameters	Values
Free layer dimension	$60 \times 60 \times 1$ nm^3
Pinned layer diameter for local injection of current	20 nm
Saturation magnetization at RT, M_{s0}	6×10^5 A/m (0.75 T)
PMA constant at RT, K_{u0}	1.5×10^6 J/m^3 (1.5×10^7 erg/cm^3)
Exchange stiffness constant (A_{ex})	1.5×10^{-11} J/m
DMI constant (D)	5.0×10^{-3} J/m^2
Damping coefficient	0.3
Polarization	0.72
Simulation mesh size	$2 \times 2 \times 1$ nm^3

used value [17], to enhance the skyrmion thermal stability and retention at room temperature (RT, 300 K). Saturation magnetization (M_s) and K_u follow the static temperature effect [26]

$$M_s(T) = M_s(0) \cdot (1 - BT^{1.5}) \tag{2}$$

and

$$\frac{K_u(T)}{K_u(0)} = [\frac{M_s(T)}{M_s(0)}]^2, \tag{3}$$

where B is *Bloch* constant estimated to be 6.17×10^{-5} K$^{-3/2}$ for Co/Pt multilayer. Note that stray fields exist in FL from PL [27], which could be reduced by properly designing the synthetic antiferromagnetic stack in MTJ [28] and are neglected for simplify. The local anisotropy variation caused by FL/BL interface as well as non-uniform distribution of current and temperature are neglected in micromagnetic simulation.

The read-out mechanism in FL is through tunneling magneto-resistance (TMR) effect. The MTJ resistance (R) depends on the angle (θ) of magnetization moments in PL and FL, expressed as [29], [30]

$$R = R_P + \frac{1}{2}(R_{AP} - R_P)(1 - \cos\theta), \tag{4}$$

with a linear variation *vs.* cosθ. Generally, with the magnetization direction of two FM layers in parallel ($\theta = 0°$) or antiparallel ($\theta = 180°$), the MTJ exhibits two resistance states R_P or R_{AP}, respectively. In this work, note that MTJ shows R_P and R_{SK}, with uniform and skyrmion state in FL, respectively (see inset of Fig. 1b).

During the heating process, the temperature evolution based on 1D model of heat diffusion [5] can be expressed as

$$T = T_{RT} + aP[1 - \exp(-\frac{t}{\tau})] \tag{5}$$

with $a = \frac{d_{TB}}{2k_{TB}A}$ and power $P = I^2R$, where d_{TB} and k_{TB} are the thickness and the thermal conductivity of TB, respectively, A is the lateral area of MTJ, and τ is thermal time constant of the entire system. Both a and τ can be tuned by TB properties (*e.g.* d_{TB} and k_{TB}). Here, we assume $a = 10^5$ K/W and $\tau = 2$ ns, which are close to that in a TA-MRAM device [5]. During natural cooling process, T is expressed as

$$T = T_{RT} + (T_0 - T_{RT}) \cdot \exp(-\frac{t}{\tau}) \tag{6}$$

where T_0 is the temperature when removing the current. Continuous temperature evolution is discretized with $\Delta t = 0.02/0.2/0.5$ ns, included in OOMMF simulation.

III. RESULTS AND DISCUSSION

A. Temperature Dependence of Uniform and Skyrmion State

Fig. 1b shows the perpendicular component of magnetization (m_z) distribution along the skyrmion diameter direction (x) at 0 K for uniform and skyrmion state. To obtain the average θ between FL with skyrmion state and PL, the average m_z ($\bar{m}_z$) in FL below PL is calculated to be $\sim$−0.3, which is equal to cosθ when the magnetization in PL keeps upward. We assume the TMR ratio, $(R_{AP} - R_P)/R_P$, is 200%, and then the resistance variation $(R_{SK} - R_P)/R_P$ is calculated to be $\sim$130% (by eq. 4). At room temperature, the magnetization and $(R_{SK} - R_P)/R_P$ are trembling with time due to the thermal fluctuation (Fig. 1c).

The magnetization evolutions within 10 ns from uniform and skyrmion state at different temperature are investigated as shown in Fig. 2. As temperature increases, uniform state changes from a single domain to multi domain (Fig. 2a–d) due to the reduced anisotropy. Regarding the skyrmion state (Fig. 2e–h), with the temperature and the thermal fluctuation increasing, skyrmion trembling becomes more intense. At high temperature ($>\sim$360 K), the skyrmion touches the boundary and then FL also changes to multi domain (Fig. 2g–h). Moreover, when the temperature goes back to RT, FL with multi domain can return to the single domain (*i.e.* uniform state) with increased anisotropy.

B. Operation of TA-SKM

Based on the results above, by heating up and cooling down, the state transition from skyrmion to uniform can be realized, denoting as RESET operation. Fig. 3a shows an example of temperature and magnetization evolutions during RESET process, induced by heating up FL to $\sim$401 K under a heat current of $I = 0.4$ mA (given $R_{SK} \sim 10$ kΩ, then

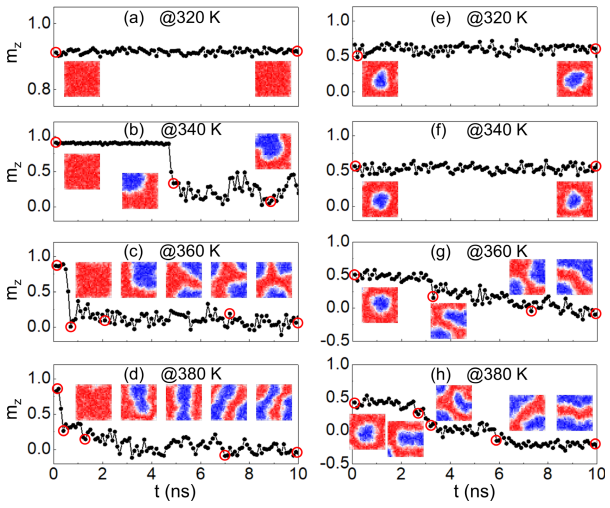

Fig. 2. (a)–(d) Magnetization evolution from uniform state at (a) 320 K, (b) 340 K, (c) 360 K, (d) 380 K. (e)–(h) Magnetization evolution from skyrmion state at (e) 320 K, (f) 340 K, (g) 360 K, (h) 380 K. Insets are the snapshots at the moments indicated by red circles. Here, m_Z is the normalized perpendicular component of magnetization in the whole FL.

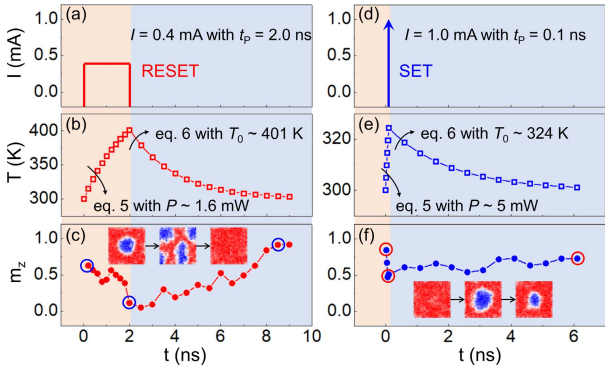

Fig. 3. (a)–(c) RESET operation. A RESET current (a) cause the temperature evolution (b) and the magnetization transition from skyrmion to uniform state by heating up FL to ~ 401 K(c). (d)–(f) SET operation. A SET current (d) cause the temperature evolution (e) and the magnetization transition from uniform to skyrmion state via STT (f).

$P \sim 1.6$ mW) for duration $t_p = 2.0$ ns and then cooling down to 300 K. On the other hand, the state transition from uniform to skyrmion, *i.e.* SET operation, is implemented by current-induced STT. Fig. 3b shows the temperature and magnetization evolutions during SET process, induced by a current of $I = 1.0$ mA (given $R_P \sim 5$ kΩ, then $P \sim 5$ mW) for $t_p = 0.1$ ns. Besides, read process is performed at much lower current within 10 ns; a small temperature increase (<20 K) is induced and will not cause the disturbance of skyrmion state.

C. Discussion of TA-SKM Performance

The switching speed of TA-SKM depends on both heating and cooling time. The natural cooling time is always close to 3τ (~6 ns here) and can be adjusted by device stack engineering [5]. Heating time is determined by the current duration required to create and destroy the skyrmion, which is small as ~0.1 and ~2 ns for SET and RESET process (Fig. 3), respectively. For skyrmion annihilation during RESET, there exists a trade-off between the current amplitude and the pulse duration. Smaller current can be adopted for optimal power consumption, while larger one for optimal switching speed. The current density of SET pulse ($\sim 3 \times 10^2$ MA/cm^2) of TA-SKM is still relatively large at this stage, because the STT-induced skyrmion nucleation from uniform FM state needs to overcome a high topological energy barrier. However, this can be further mitigated by adopting materials with low damping [17] or by tuning the offset stray filed in FL from the PL stack [31]. TA-SKM device can be scaled down with the skyrmion size and the stacked MTJ. The skyrmion diameter is related to the magnetic parameters, which can be sub-10 nm theoretically [17], ensuring the scalability of the proposed device. In addition, the retention of skyrmion state at 300 K is limited (estimated to be ms level under our parameters). Therefore, the proposed TA-SKM prefers to the applications for DRAM or last-level cache (LLC) replacement.

Compared to the STT-MRAM, TA-SKM has similar read operation to obtain the stored MR state of MTJ. The sensing margin in TA-SKM is degraded due to the reduced TMR ratio at the same barrier oxide thickness of MTJ. However, for STT-MRAM, TMR needs to be large for increasing read margin, while resistance-area (RA) value needs to be small for reducing STT write power/voltage. Due to the un-decoupled read and write paths, TMR and RA are strong trade-offs in STT-MRAM. By contrast, because the write operation in TA-SKM now can be assisted by JHE, its reliance on STT is reduced as compared to STT-MRAM, indicating that higher TMR or RA design can be used for MTJ in TA-SKM to increase the read margin. Furthermore, while STT-MRAM uses bidirectional currents/STT for FL's magnetization switching, TA-SKM uses only unidirectional currents for skyrmion creation and annihilation. Unipolar switching in TA-SKM could potentially simplify the selector device option and circuit design. One-diode/selector-one-memory (1D/S1M) structure can be used instead of one-transistor-one-memory (1T1M). For example, TA-SKM can cooperate with unipolar poly-Si-based diode with on-current density of 10^7-10^8 A/cm^2 and low off-current density [32], instead of the more exotic selectors like Ovonic Threshold Switch [33], for high-density cross-point memory integrations.

On the other hand, conventional TA-MRAM requires to increase temperature by more than 200 K during operation, which risks the degradation of tunnel junctions under heat current pulses and the disturbance of unselected cells due to thermal cross-talk at array level. In our proposed TA-SKM, however, the elevated temperature during operation is about 100 K or less, which is expected to have better reliability for high-density memories.

IV. Conclusion

A novel TA-SKM memory device has been proposed based on MTJ structure with DMI in FL sandwiched by thermal barriers. Unidirectional current-induced both STT and JHE are used to alter the magnetization in FL between skyrmion and uniform state, thus the switching of the resistance states between R_{SK} and R_P. TA-SKM has potential improvements in TMR design, selector device/circuit options, operation temperature range, as compared to STT- and TA-MRAMs. Furthermore, this work paves a new insight for spintronics and topological magnetism communities by exploiting the thermal properties and applications of magnetic skyrmion.

REFERENCES

[1] X. Fong, Y. Kim, R. Venkatesan, S. H. Choday, A. Raghunathan, and K. Roy, "Spin-transfer torque memories: Devices, circuits, and systems," *Proc. IEEE*, vol. 104, no. 7, pp. 1449–1488, Jul. 2016, doi: 10.1109/JPROC.2016.2521712.

[2] Y. J. Song, J. H. Lee, H. C. Shin, K. H. Lee, K. Suh, J. R. Kang, S. S. Pyo, H. T. Jung, S. H. Hwang, G. H. Koh, S. C. Oh, S. O. Park, J. K. Kim, J. C. Park, J. Kim, K. H. Hwang, G. T. Jeong, K. P. Lee, and E. S. Jung, "Highly functional and reliable 8Mb STT-MRAM embedded in 28 nm logic," in *IEDM Tech. Dig.*, Dec. 2016, pp. 27.2.1–27.2.4, doi: 10.1109/IEDM.2016.7838491.

[3] N. Xu, P.-Y. Chen, J. Wang, W. Choi, K.-H. Lee, E. S. Jung, and S. Yu, "Review of physics-based compact models for emerging non-volatile memories," *J. Comput. Electron.*, vol. 16, no. 4, pp. 1257–1269, Dec. 2017, doi: 10.1007/s10825-017-1098-0.

[4] I. L. Prejbeanu, M. Kerekes, R. C. Sousa, H. Sibuet, O. Redon, B. Dieny, and J. P. Nozières, "Thermally assisted MRAM," *J. Phys., Condens. Matter*, vol. 19, no. 16, Apr. 2007, Art. no. 165218, doi: 10.1088/0953-8984/19/16/165218.

[5] C. Papusoi, R. Sousa, J. Herault, I. L. Prejbeanu, and B. Dieny, "Probing fast heating in magnetic tunnel junction structures with exchange bias," *New J. Phys.*, vol. 10, no. 10, Oct. 2008, Art. no. 103006, doi: 10.1088/1367-2630/10/10/103006.

[6] S. Bandiera, R. C. Sousa, M. M. de Castro, C. Ducruet, C. Portemont, S. Auffret, L. Vila, I. L. Prejbeanu, B. Rodmacq, and B. Dieny, "Spin transfer torque switching assisted by thermally induced anisotropy reorientation in perpendicular magnetic tunnel junctions," *Appl. Phys. Lett.*, vol. 99, no. 20, Nov. 2011, Art. no. 202507, doi: 10.1063/1.3662971.

[7] M. H. Kryder, E. C. Gage, T. W. McDaniel, W. A. Challener, R. E. Rottmayer, G. Ju, Y.-T. Hsia, and M. F. Erden, "Heat assisted magnetic recording," *Proc. IEEE*, vol. 96, no. 11, pp. 1810–1835, Nov. 2008, doi: 10.1109/JPROC.2008.2004315.

[8] C. Vogler, C. Abert, F. Bruckner, D. Suess, and D. Praetorius, "Heat-assisted magnetic recording of bit-patterned media beyond 10 Tb/in^2," *Appl. Phys. Lett.*, vol. 108, no. 10, Mar. 2016, Art. no. 102406, doi: 10.1063/1.4943629.

[9] M. C. Kautzky and M. G. Blaber, "Materials for heat-assisted magnetic recording heads," *MRS Bull.*, vol. 43, no. 2, pp. 100–105, Feb. 2018, doi: 10.1557/mrs.2018.1.

[10] W. Kang, Y. Huang, X. Zhang, Y. Zhou, and W. Zhao, "Skyrmion-electronics: An overview and outlook," *Proc. IEEE*, vol. 104, no. 10, pp. 2040–2061, Oct. 2016, doi: 10.1109/jproc.2016.2591578.

[11] K. Everschor-Sitte, J. Masell, R. M. Reeve, and M. Kläui, "Perspective: Magnetic skyrmions—Overview of recent progress in an active research field," *J. Appl. Phys.*, vol. 124, no. 24, Dec. 2018, Art. no. 240901, doi: 10.1063/1.5048972.

[12] W. Jiang, G. Chen, K. Liu, J. Zang, S. G. E. Te Velthuis, and A. Hoffmann, "Skyrmions in magnetic multilayers," *Phys. Rep.*, vol. 704, pp. 1–49, Aug. 2017, doi: 10.1016/j.physrep.2017.08.001.

[13] S. Luo, N. Xu, Z. Guo, Y. Zhang, J. Hong, and L. You, "Voltage-controlled skyrmion memristor for energy-efficient synapse applications," *IEEE Electron Device Lett.*, vol. 40, no. 4, pp. 635–638, Apr. 2019, doi: 10.1109/LED.2019.2898275.

[14] Z. Zhang, Y. Zhu, Y. Zhang, K. Zhang, J. Nan, Z. Zheng, Y. Zhang, and W. Zhao, "Skyrmion-based ultra-low power electric-field-controlled reconfigurable (SUPER) logic gate," *IEEE Electron Device Lett.*, vol. 40, no. 12, pp. 1984–1987, Dec. 2019, doi: 10.1109/LED.2019.2946863.

[15] S. Luo, M. Song, X. Li, Y. Zhang, J. Hong, X. Yang, X. Zou, N. Xu, and L. You, "Reconfigurable Skyrmion logic gates," *Nano Lett.*, vol. 18, no. 2, pp. 1180–1184, Feb. 2018, doi: 10.1021/acs.nanolett.7b04722.

[16] N. Romming, C. Hanneken, M. Menzel, J. E. Bickel, B. Wolter, K. von Bergmann, A. Kubetzka, and R. Wiesendanger, "Writing and deleting single magnetic skyrmions," *Science*, vol. 341, no. 6146, pp. 636–639, Aug. 2013, doi: 10.1126/science.1240573.

[17] J. Sampaio, V. Cros, S. Rohart, A. Thiaville, and A. Fert, "Nucleation, stability and current-induced motion of isolated magnetic skyrmions in nanostructures," *Nature Nanotechnol.*, vol. 8, no. 11, pp. 839–844, Nov. 2013, doi: 10.1038/nnano.2013.210.

[18] W. Koshibae and N. Nagaosa, "Creation of skyrmions and antiskyrmions by local heating," *Nature Commun.*, vol. 5, no. 1, p. 5148, Dec. 2014, doi: 10.1038/ncomms6148.

[19] G. Berruto, I. Madan, Y. Murooka, G. M. Vanacore, E. Pomarico, J. Rajeswari, R. Lamb, P. Huang, A. J. Kruchkov, Y. Togawa, T. LaGrange, D. McGrouther, H. M. Rønnow, and F. Carbone, "Laser-induced skyrmion writing and erasing in an ultrafast cryo-lorentz transmission electron microscope," *Phys. Rev. Lett.*, vol. 120, no. 11, Mar. 2018, Art. no. 117201, doi: 10.1103/PhysRevLett.120.117201.

[20] S. Rohart and A. Thiaville, "Skyrmion confinement in ultrathin film nanostructures in the presence of Dzyaloshinskii-Moriya interaction," *Phys. Rev. B, Condens. Matter*, vol. 88, no. 18, Nov. 2013, Art. no. 184422, doi: 10.1103/PhysRevB.88.184422.

[21] M. K. Samani, X. Z. Ding, N. Khosravian, B. Amin-Ahmadi, Y. Yi, G. Chen, E. C. Neyts, A. Bogaerts, and B. K. Tay, "Thermal conductivity of titanium nitride/titanium aluminum nitride multilayer coatings deposited by lateral rotating cathode arc," *Thin Solid Films*, vol. 578, pp. 133–138, Mar. 2015, doi: 10.1016/j.tsf.2015.02.032.

[22] M. J. Donahue and D. G. Porter, "OOMMF user's guide," Nat. Inst. Standards Technol., Gaithersburg, MD, USA, Interagency Rep. 6376. Jan. 1999. [Online]. Available: http://math.nist.gov/oommf

[23] *Xf_ThermSpinXferEvolve | Kelvinxyfong*. Accessed: Mar. 17, 2014. [Online]. Available: http://kelvinxyfong.wordpress.com/research/research-interests/oommf-extensions/oommf-extension-xf_thermspinxferevolve

[24] X. Zhang, M. Ezawa, and Y. Zhou, "Thermally stable magnetic skyrmions in multilayer synthetic antiferromagnetic racetracks," *Phys. Rev. B, Condens. Matter*, vol. 94, no. 6, Aug. 2016, Art. no. 064406, doi: 10.1103/PhysRevB.94.064406.

[25] J. Wild, T. N. G. Meier, S. Pöllath, M. Kronseder, A. Bauer, A. Chacon, M. Halder, M. Schowalter, A. Rosenauer, J. Zweck, J. Müller, A. Rosch, C. Pfleiderer, and C. H. Back, "Entropy-limited topological protection of skyrmions," *Sci. Adv.*, vol. 3, no. 9, Sep. 2017, Art. no. e1701704, doi: 10.1126/sciadv.1701704.

[26] M. Song, Y. Xu, J. OuYang, Y. Zhang, D. Liu, X. Yang, X. Zou, and L. You, "Low current writing perpendicular magnetic random access memory with high thermal stability," *Mater. Des.*, vol. 92, pp. 1046–1051, Feb. 2016, doi: 10.1016/j.matdes.2015.12.092.

[27] Z. Zhao, A. K. Smith, M. Jamali, and J.-P. Wang, "External-field-free spin Hall switching of perpendicular magnetic nanopillar with a dipole-coupled composite structure," 2016, *arXiv:1603.09624*. [Online]. Available: http://arxiv.org/abs/1603.09624

[28] Y.-H. Wang, S.-H. Huang, D.-Y. Wang, K.-H. Shen, C.-W. Chien, K.-M. Kuo, S.-Y. Yang, and D.-L. Deng, "Impact of stray field on the switching properties of perpendicular MTJ for scaled MRAM," in *IEDM Tech. Dig.*, Dec. 2012, pp. 29.2.1–29.2.4, doi: 10.1109/IEDM.2012.6479127.

[29] Y. Zhang, B. Yan, J. Ou-Yang, X. Wang, B. Zhu, S. Chen, and X. Yang, "Significant manipulation of output performance of a bridge-structured spin valve magnetoresistance sensor via an electric field," *J. Appl. Phys.*, vol. 119, no. 4, Jan. 2016, Art. no. 044101, doi: 10.1063/1.4940360.

[30] H. Chen, M. Song, Z. Guo, R. Li, Q. Zou, S. Luo, S. Zhang, Q. Luo, J. Hong, and L. You, "Highly secure physically unclonable cryptographic primitives based on interfacial magnetic anisotropy," *Nano Lett.*, vol. 18, no. 11, pp. 7211–7216, Nov. 2018, doi: 10.1021/acs.nanolett.8b03338.

[31] X. Zhang, W. Cai, X. Zhang, Z. Wang, Z. Li, Y. Zhang, K. Cao, N. Lei, W. Kang, Y. Zhang, H. Yu, Y. Zhou, and W. Zhao, "Skyrmions in magnetic tunnel junctions," *ACS Appl. Mater. Interfaces*, vol. 10, no. 19, pp. 16887–16892, May 2018, doi: 10.1021/acsami.8b03812.

[32] M. Kinoshita, Y. Sasago, H. Minemura, Y. Anzai, M. Tai, Y. Fujisaki, S. Kusaba, T. Morimoto, T. Takahama, T. Mine, A. Shima, Y. Yonamoto, and T. Kobayashi, "Scalable 3-D vertical chain-cell-type phase-change memory with 4F2 poly-Si diodes," in *Proc. Symp. VLSI Technol. (VLSIT)*, Jun. 2012, pp. 35–36, doi: 10.1109/VLSIT.2012.6242448.

[33] Y. Koo, S. Lee, S. Park, M. Yang, and H. Hwang, "Simple binary ovonic threshold switching material SiTe and its excellent selector performance for high-density memory array application," *IEEE Electron Device Lett.*, vol. 38, no. 5, pp. 568–571, May 2017, doi: 10.1109/LED.2017.2685435.